

# Dielectric Properties of Cellulose Acylates

TOSHIRO MOROOKA, MISATO NORIMOTO, and TADASHI YAMADA,  
*Wood Research Institute, Kyoto University, Uji, Kyoto 611, Japan, and*  
NOBUO SHIRAIISHI, *Faculty of Agriculture, Kyoto University, Sakyo-ku,*  
*Kyoto 606, Japan*

## Synopsis

Thirteen kinds of cellulose acylates from the acetate to stearate were prepared by trifluoro acetic anhydride-fatty acid esterification, and their dielectric constant and loss were measured over wide temperature and frequency ranges. Two types of relaxation process ( $\alpha_d$  and  $\beta_d$ ) were recognized for all the acylates and an additional relaxation process ( $\gamma_d$ ) was detected for the acylates with side chain length longer than that of the butyrate. These  $\alpha_d$  to  $\gamma_d$  processes were attributed to the micro-Brownian motion of the main chain ( $\alpha_d$ ), the motion of oxycarbonyl group of the side chain ( $\beta_d$ ) and the motion initiated by minimum three methylene groups in addition to the oxycarbonyl group ( $\gamma_d$ ), respectively. In the transition map for the  $\beta_d$  process, inflection points were observed, and the temperature at the inflection point could be regarded as a freezing point of the micro-Brownian motion of the acyl side chain. In the temperature region above the inflection point, plots in transition map for all the acylates were found to be on the same straight line.

## INTRODUCTION

One of the useful procedures for assigning the molecular relaxation processes of polymers is through altering chemical constituents systematically. In line with this, many types of side chains were introduced systematically in the synthetic polymers such as polymethacrylates or polyacrylates, and their relaxation mechanisms were investigated.<sup>1,2</sup> Poly(*n*-alkyl methacrylate)s, in particular, have been studied extensively by using mechanical or dielectric measurements. In this case, however, the glass transition (primary process) overlaps the secondary transition (secondary process), which is due mainly to the side chain motion, for a homologue with the side chain length longer than that for poly(*n*-butylmethacrylate).<sup>3</sup> This overlapping seems to arise from the similarity in both flexibility and motional unit of the main and side chains. However, the situation is quite different for cellulose acylates, though *n*-alkyl groups are introduced in the side chain as in poly(*n*-alkyl methacrylate)s. In this case, the flexibility of the main chain is thought to be more restricted than that of the side chain, because the former consists of bulky glucopyranose units. From this, it can be expected that the primary and secondary processes for the acylates with a long side chain appear separately, so that it seems that a systematic study on the relaxation mechanism for the acylates is worth carrying out.

In the previous article,<sup>4</sup> viscoelastic properties of the acylates from propionate to decanoate were studied by using dynamic mechanical measurements at low frequencies in the temperature range from  $-190^{\circ}\text{C}$  to  $200^{\circ}\text{C}$ .

Four types of relaxation process were observed for the acylates from butyrate to hexanoate, being labelled  $\alpha_m, \beta_m, \beta'_m$ , and  $\gamma_m$  in order of decreasing temperature at which they were detected. However, the  $\gamma_m$  process for propionate and the  $\beta'_m$  process for decanoate were not observed. On the contrary, a relaxation process, labelled  $\gamma'_m$ , for propionate was detected. These  $\alpha_m$  to  $\gamma'_m$  processes were attributed, respectively, to the micro-Brownian motion of the main chain ( $\alpha_m$ ), the motion of the side chain ( $\beta_m$  and  $\beta'_m$ ), the motion initiated by three or more methylene groups ( $\gamma_m$ ), and the motion of two methylene groups ( $\gamma'_m$ ).

The present article describes dielectric relaxation processes of 13 kinds of the acylates from the acetate to stearate. All the samples employed in this experiment are prepared by trifluoro acetic anhydride–fatty acid esterification, which is considered to be suitable for our experiments, since it induces no notable cellulose degradation and results in pure and colorless products.

## EXPERIMENTAL

**Materials.** The cellulose used was Whatman cellulose powder CF-11. Special grade trifluoro acetic anhydride (TFAA) and *n*-fatty acids; propionic acid, butyric acid, valeric acid, hexanoic acid, enanthic acid, octanoic acid, peralgonic acid, decanoic acid, lauric acid, myristic acid, palmitic acid, and stearic acid were used for the acylation of cellulose. Reagent grade methanol was used as a precipitant.

**Preparation of Cellulose Acylates.** TFAA (16.7 mL/g of cellulose) and the corresponding fatty acids from acetic to *n*-stearic acid (mole ratio of fatty acid to TFAA was 1.23) were mixed together and stirred mildly at 50°C for 20 min to increase the aging (formation of the mixed acid anhydride). This solution was added to dried cellulose powder (6 g) placed in a 300-mL Erlenmyer flask equipped with a condenser and stirred mildly at 50°C for 5 h. The reaction mixture was poured into an excess amount of methanol, and the precipitates were filtered and washed with methanol repeatedly.

**Characterization.** The weight-average molecular weight of the sample was determined by the use of a gel permeation chromatography (Shimazu GPC-700) in which tetrahydrofuran was used as a solvent. The degree of substitution was estimated by both the saponification method and infrared (IR) spectrometry. The KBr disc technique was employed in IR spectrometry.

**Measurement of Melting.** Melting of the acylates was observed by using a thermomechanical analyzer (TMA)<sup>5</sup> (Shinku Riko Co. Ltd., TM-1500), in which a column of the sample collapsed under a plunger which supported a constant load of 3 kg/cm<sup>2</sup>, when heated at a uniform rate of 1°C/min. It was also followed by optical micrographic observation.

**Dielectric Measurements.** The powdered samples pressed into uniform compact discs 5 cm in diameter and 0.7 mm in thickness were used for dielectric measurements. Using a transformer bridge (Ando Denki, TR-10C), dielectric constant and dielectric loss were measured over the frequency range of 50 Hz to 1.0 MHz and the temperature range of –190 to 200°C.

TABLE I  
Characteristics of the Acylates Used

| Acylates    | $n$ | DS   | $M_w$              | $T_m$ (°C) |
|-------------|-----|------|--------------------|------------|
| Acetate     | 2   | 2.83 | —                  | 278        |
| Propionate  | 3   | 2.96 | $1.48 \times 10^5$ | 241        |
| Butyrate    | 4   | 2.80 | $1.77 \times 10^5$ | 189        |
| Valerate    | 5   | 2.79 | $2.15 \times 10^5$ | 128        |
| Hexanoate   | 6   | 2.83 | $2.15 \times 10^5$ | 110        |
| Enanthate   | 7   | 3.04 | $2.07 \times 10^5$ | 103        |
| Octanoate   | 8   | 2.84 | $2.03 \times 10^5$ | 93         |
| Pelargonate | 9   | —    | $3.54 \times 10^5$ | 87         |
| Decanoate   | 10  | —    | $2.32 \times 10^5$ | 102        |
| Laurate     | 12  | —    | $2.18 \times 10^5$ | 112        |
| Myristate   | 14  | —    | $2.87 \times 10^5$ | 108        |
| Palmitate   | 16  | —    | $3.98 \times 10^5$ | 113        |
| Stearate    | 18  | —    | $6.91 \times 10^5$ | 121        |

## RESULTS AND DISCUSSION

Table I shows the number of carbons introduced in the acyl side chain,  $n$ , the degree of substitution, DS, the average molecular weight  $M_w$ , and the melting point  $T_m$  for a series of cellulose acylates from the acetate to the stearate prepared. The  $M_w$  values are of the order of about  $10^5$ . The values of DS determined by saponification method for the acylates up to  $n=8$  exceed about 2.8. However, determination of DS by using saponification method became inaccurate for the acylates above  $n=9$ . Therefore, instead of saponification method, DS of the samples above  $n=9$  was estimated by IR spectrometry.

Figure 1 shows IR spectra for the valerate to the stearate. Absorption

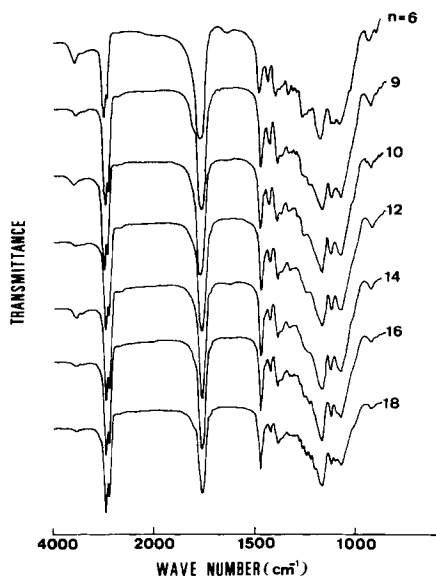


Fig. 1. Infrared spectra of the acylates;  $n$  = the number of carbon in the acyl side chain.

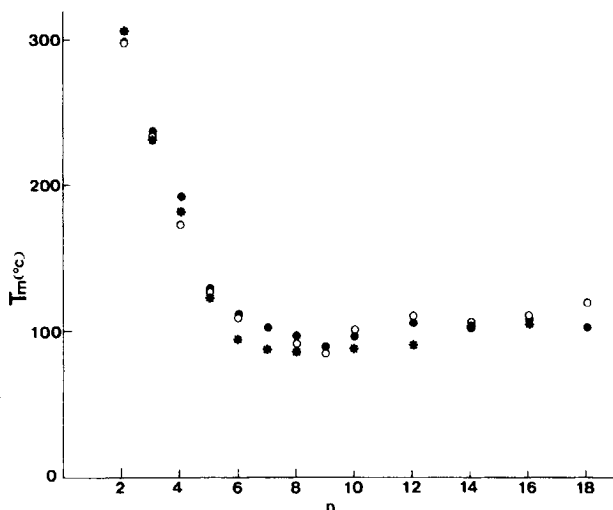


Fig. 2. Dependence of the melting point ( $T_m$ ) on the number of carbons ( $n$ ) in the acyl side chain: (○) micrographic observation; (●) TMA; (\*) after Malm et al.<sup>6</sup>

intensity of OH stretching band in the vicinity of  $3600\text{ cm}^{-1}$  for the acylates above  $n=9$  is smaller than that for the valerate whose DS value is 2.79. From these results, all the acylates prepared are thought to be almost fully acylated.

In order to define  $T_m$  of the sample, comparisons of the temperatures were made as determined by the following two types of measurements. One way is measuring the temperature  $T_{m1}$ , at which the samples when heated at a constant rate became quickly transparent under microscopic observation. The second process is measuring the temperature  $T_{m2}$  at which the plunger in TMA reached the bottom of the glass capillary, indicating transition from solid state to liquid state. Both temperatures thus obtained coincided closely. Therefore, in this report, both  $T_{m1}$  and  $T_{m2}$  can be used as  $T_m$ . In the table,  $T_{m1}$  is shown as of the sample.

Figure 2 shows the variation of  $T_m$  ( $T_{m1}, T_{m2}$ ) with  $n$  for the acylates. The values of  $T_m$  decrease abruptly with increasing  $n$  up to 5, i.e., they fall from  $300^\circ\text{C}$  to  $128^\circ\text{C}$  as  $n$  increased from 2 to 5. However, even if additional acyl methylene units were added in the formation of the higher homologues ( $n=6$  or higher),  $T_m$  remains almost unchanged. In the same figure, the results of the acylates prepared by Malm et al.<sup>6</sup> by using acid chloride-pyridine esterification are also shown. Obviously, they are in fair agreement with those of our samples.

For the acylates thus characterized, dielectric relaxation experiments were carried out. Figures 3 and 4 give variation of the dielectric loss  $\epsilon''$  for the valerate and the palmitate, respectively, as a function of the temperature and frequency, i.e., contour diagrams. In these figures, three types of relaxation process can be recognized, which are labelled  $\alpha_d$ ,  $\beta_d$ , and  $\gamma_d$  in order of decreasing temperature or in order of increasing frequency at which they were detected. Also, for the butyrate to the stearate three relaxation processes ( $\alpha_d$ ,  $\beta_d$ , and  $\gamma_d$ ) similar to those for the valerate or the palmitate are obtained. However, the  $\alpha_d$  process for the acetate and  $\gamma_d$

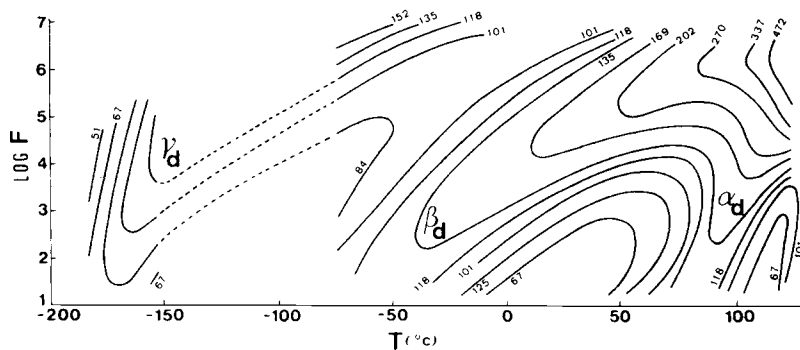


Fig. 3. Contour diagrams of the dielectric loss  $\epsilon''$  for the valerate as a function of logarithmic frequency ( $F$ ) and temperature ( $T$ ).  $\epsilon''$  value given in units of  $10^{-4}$ .

process for both acetate and propionate are not observed. On the contrary, a relaxation process, labelled  $\gamma'_d$ , is detected for the propionate. It should be emphasized that the  $\alpha_d$  and the  $\beta_d$  processes are observed separately in the contour diagrams even for the acylates having a side chain with length long enough as in the stearate; this is quite different from the case of poly( $n$ -alkyl methacrylate).<sup>3</sup> In the following, the molecular mechanism for these  $\alpha_d$  to  $\gamma_d$  processes will be discussed, in sequence, in relation to the mechanical relaxation processes ( $\alpha_m, \beta_m, \gamma_m$ , and  $\gamma'_m$ ) previously reported.

The  $\alpha_d$  process is observed in the higher temperature and in the lower frequency region prior to the melting of the sample (Figs. 3 and 4). Regarding the  $\alpha_d$  process, the value of apparent activation energy  $\Delta E$  for  $n$  from 3 to 6 decreases with increasing  $n$ , i.e., 160, 67, 58, and 50 kcal/mol, respectively, but, for  $n$  above 6, it remains at a constant value of about 50 kcal/mol. In connection with the  $\alpha_d$  process, Mikhailov et al.<sup>7</sup> found a process, having a  $\Delta E$  of 70 kcal/mol for the acetate at a frequency of 10 kHz at 220°C by using dielectric measurements. Judging from both the temperature–frequency location and the  $\Delta E$  value, this process can be classified as the  $\alpha_d$  process. Therefore, the  $\alpha_d$  process is thought to appear in all the acylates examined. Corresponding to this, the location of the  $\alpha_d$  process for each

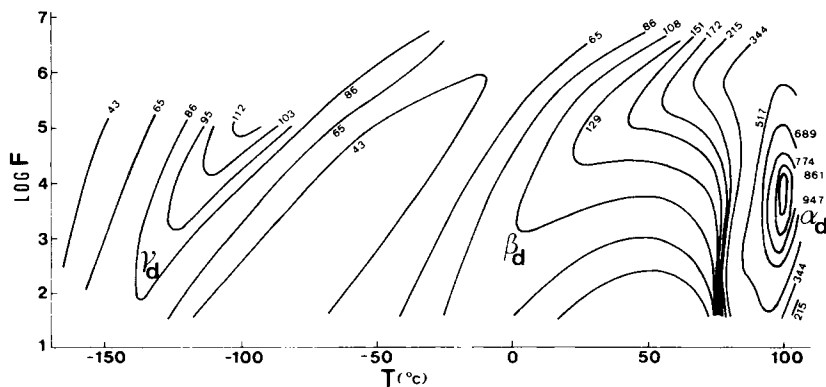


Fig. 4. Contour diagrams of the dielectric loss  $\epsilon''$  for the palmitate as a function of logarithmic frequency ( $F$ ) and temperature ( $T$ ).  $\epsilon''$  value given in units of  $10^{-4}$ .

acylate is comparable to that of the  $\alpha_m$  process described above. From these findings, the  $\alpha_d$  process as well as the  $\alpha_m$  process are considered due to the micro-Brownian motion of the main chain. Thus, the  $\alpha_d$  process is related to the glass-rubber transition of the acylates. Accordingly, the temperature location of  $\epsilon''$  maximum at a low frequency for the  $\alpha_d$  process can be regarded as a rough measure of the glass transition point  $T_g$  of the sample. As was observed in the  $\alpha_m$  absorption at a low frequency, the  $T_g$  thus defined shifts markedly with increasing  $n$  up to 6. This phenomenon can be interpreted as follows: the increase in the molecular size of nonpolar  $n$ -alkyl groups causes a decrease in the interaction of dipolar ester groups, thus facilitating the chain backbone motion. This effect is similar to that produced by the addition of a plasticizer. However, the  $T_g$  seems to level off when  $n$  reached 6. These trends recognized for  $T_g$  are parallel to those for the melting points of the sample (Fig. 2). On the other hand, it has been reported that the  $T_g$  for poly( $n$ -alkyl methacrylate)s decreases continuously with increasing  $n$ , reaching  $-65^\circ\text{C}$  for poly( $n$ -dodecyl methacrylate).<sup>8</sup> This difference between cellulose acylate and poly( $n$ -alkyl methacrylate), both involving long  $n$ -alkyl groups in the side chain, may be attributed to the different structure of the main chain; the former is bulkier than the latter.

As the acetyl content in cellulose increases, the relaxation process due to the orientation of methylol groups becomes less distinct, but, instead, the  $\beta_d$  process appears.<sup>9</sup> Many investigators have reported on the  $\beta_d$  process in acetate,<sup>10-14</sup> and they attributed this process mainly to the hindered rotation of the acetyl group. As stated above, however, it should be noted that the  $\beta_d$  process is recognized not only for the acetate but also for all the acylates examined. This fact means that the  $\beta_d$  process reflects motions within the acyl groups. In order to assign the  $\beta_d$  process, plots of logarithmic frequency  $F_m$  at  $\epsilon''$  maximum against the reciprocal of the absolute temperature  $T^{-1}$ , i.e., transition map, for all the acylates are shown in Figure 5. In the figure, several plots which are discussed in a later paragraph are

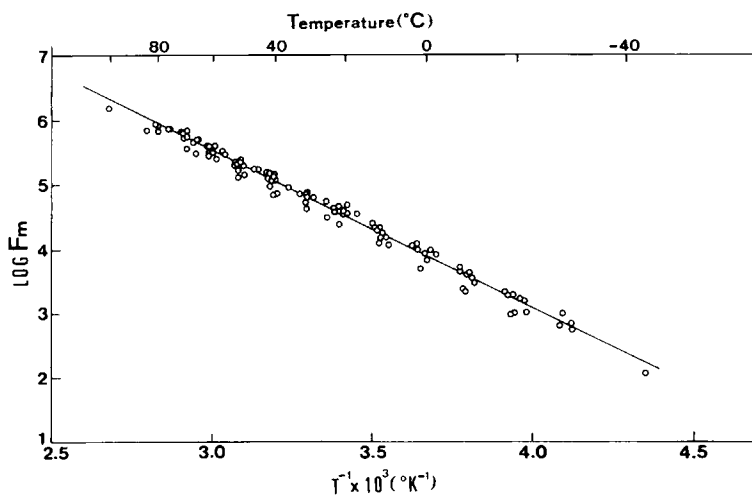


Fig. 5. Plots of logarithmic frequency ( $F_m$ ) at  $\epsilon''$  maximum against reciprocal of the absolute temperature  $T^{-1}$  for the  $\beta_d$  process.

TABLE II  
 $\Delta E$ ,  $\Delta S$ , and  $\Delta F$  for Cellulose and the Acylates

| Samples <sup>a</sup> | Relaxation   | $\Delta E$ (kcal/mol) | $\Delta S$ (e. u.) | $\Delta F$ (kcal/mol) |
|----------------------|--|-----------------------|--------------------|-----------------------|
| Cellulose            | $\left\{ \begin{array}{l} \text{I} \\ \text{II} \end{array} \right.$<br>$\text{CH}_2\text{OH}$ Group | 10.1                  | 9.3-10.2           | 7.5-8.0               |
|                      |  | 10.6                  | 9.8-10.4           | 7.6-8.2               |
| Acylates             | $\beta_d$ $n = 2-18$   | 11.3                  | 0.7-3.6            | 9.7-10.4              |

<sup>a</sup> Cellulose I = Whatman cellulose CF-11; cellulose II, prepared by saponification of the acetate.

not included. It is noted that all the resulting plots are on one straight line. By means of the least square method, this line is expressed by the equation,

$$\log F_m = -2459T^{-1} + 12.91 \quad (1)$$

with a correlation coefficient of 0.994. The  $\Delta E$  value calculated is 11.3 kcal/mol, which is comparable to that reported for the  $\beta_d$  of the acetate.<sup>10,12,13</sup> The finding that the  $\beta_d$  process for all the acylates gives the same  $\Delta E$  and relaxation time means that this process results from a dielectrically active common unit in the acyl side chain. Such a unit is the oxycarbonyl groups attached to the glucopyranose ring. Thus, it is concluded that the  $\beta_d$  process can be regarded as due to the orientational polarization of the oxycarbonyl group in the side chain.

Concerning the acetate, however, our conclusion does not necessarily contradict the assignments proposed by other investigators. Since the acetyl side chain is substantially small in molecular size, the motion of oxycarbonyl groups in the acetyl side chain cannot be distinguished from that of the acetyl side chain itself. In fact, for the acetate the  $\beta_m$  process due to the side chain motion was detected in the temperature and frequency ranges comparable to those for the  $\beta_d$  process.<sup>15</sup> Hence, the  $\beta_d$  process can be approximately attributed to the motion of the side chain when it is small enough as in the acetate.

Table II shows  $\Delta E$ , apparent activation entropy  $\Delta S$ , and apparent activation free energy  $\Delta F$  for both the  $\beta_d$  process of cellulose acylate and the process due to the motion of methylol group of celluloses (I and II). Apparently, the value of  $\Delta E$  for the two types of molecular relaxation is the same. However, the  $\Delta S$  value for the  $\beta_d$  relaxation is small as compared to that for the relaxation of the  $-\text{CH}_2\text{OH}$  group. This indicates that the motion of the oxycarbonyl group is somewhat restricted as compared to that of the methylol group; this corresponds to the fact that the former appears in the higher temperature and lower frequency regions than the latter.

In order to obtain further information on the  $\beta_d$  process, the transition map for the acylates above  $n=12$  is shown in Figure 6, in which several plots omitted in the Figure 5 are also included. Plots for each sample in the lower temperatures which were not on the line expressed by the eq. (1) described above, instead, are lines with greater slope than the line (1). In the figure, the temperatures at the intersecting points  $T_0$  between the line (1) and the other lines are denoted by arrows. The  $T_0$  apparently shifts to a higher temperature region with increasing  $n$ , being  $-15$ ,  $12$ ,  $27$ , and  $34^\circ\text{C}$

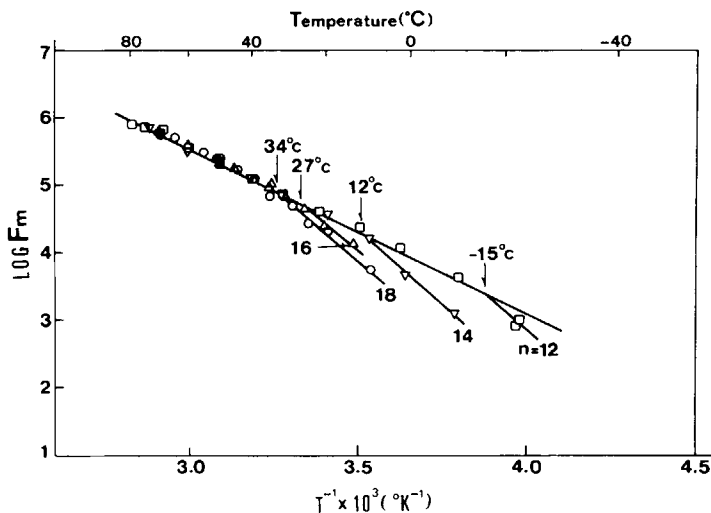


Fig. 6. Plots of logarithmic frequency ( $F_m$ ) at  $\epsilon''$  maximum against reciprocal of the absolute temperature  $T^{-1}$  for the  $\beta_d$  process for the samples  $n=12$  and above.

for  $n$  of 12, 14, 16, and 18, respectively. This phenomenon is analogous to the dependence of the glass transition temperature on the molecular weight. The  $\Delta E$  at the respective acylate in the temperature region below  $T_0$  becomes somewhat larger than that above  $T_0$ , ranging from 18.6 to 20.4 kcal/mol. This suggests that the orientation motion of the oxycarbonyl group becomes restricted in the temperature range below  $T_0$ . Although the  $\beta_m$  process as well as  $\beta'_m$  are not identical in relaxation mechanism with the  $\beta_d$  process, the results of the corresponding dynamic mechanical measurements<sup>4</sup> are available, in order to understand this phenomenon.

In the case of the cellulose decanoate ( $n=10$ ), the region in which  $\beta_m$  occurred was at the temperature of about  $-60^\circ\text{C}$  and at the frequency of 11 Hz. This process was considered to reflect a micro-Brownian motion of the side chain. Therefore, the freezing temperature of the side chain for  $n=10$  can be thought to be about  $-60^\circ\text{C}$ . On the other hand, when the relationship between  $n$  and  $T_0$  is extrapolated into the case of  $n=10$ ,  $T_0$  could be estimated to be  $-60^\circ\text{C}$ . These findings indicate  $T_0$  to be the freezing temperature of the micro-Brownian motion of the acyl side chain. Supposing that the side chain froze in the temperature region below  $T_0$ , then the orientation of the oxycarbonyl group which is a part of the side chain will be restricted. Hence, the  $\Delta E$  value below  $T_0$  becomes larger than that above  $T_0$ .

The last part of this paper is devoted to a discussion of the  $\gamma_d$  process. As was shown in Figures 3 and 4, the  $\gamma_d$  process is detected in the lowest temperature and the highest frequency region examined. The  $\gamma_d$  peak decreases gradually in height with an increase in  $n$ . However, this process is not observed for samples with  $n=2$  or 3, corresponding to the results of the  $\gamma_m$  process for the same samples. Figure 7 shows the transition map for  $\gamma_d$  above  $n=4$ . The resulting plots for each acylate are expressed by a straight line and the  $\Delta E$  value ranges from 5 to 8 kcal/mol. For  $n$  up to 7, lines are



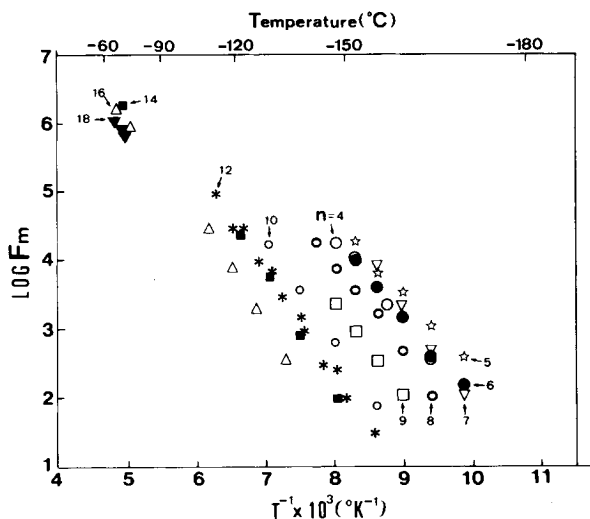


Fig. 7. Plots of logarithmic frequency ( $F_m$ ) at  $\epsilon''$  maximum against reciprocal of the absolute temperature  $T^{-1}$  for the  $\gamma_d$  process.

similar in location, but for  $n$  above 8 they move to higher temperature with increasing  $n$ . The temperature-frequency location and the  $\Delta E$  value for the  $\gamma_d$  process are comparable to those for the  $\gamma_m$  process. Accordingly, it is considered that both the  $\gamma_d$  and the  $\gamma_m$  processes are associated with the same molecular relaxation. In the previous investigation,<sup>4</sup> the  $\gamma_m$  process was ascribed to the motion initiated by three or more methylene groups in the side chain. However, since methylene groups are nonpolar, the motion of the dipolar oxycarbonyl group adjacent to the methylene groups has to be included in the  $\gamma_d$  process. From this, both the  $\gamma_d$  and  $\gamma_m$  processes are thought to be due to the motion of three or more methylene groups including the motion of the oxycarbonyl group in the side chain.

In this connection, the relaxation process which involves the motion of dipolar component in addition to those of the three or more methylene groups have been already reported for many synthetic polymers including poly( $n$ -alkyl acrylate), poly(vinyl ester)s, polyamids, and oxide polymers.<sup>1</sup> However, our systematic experiments indicate that the  $\gamma_d$  process should be regarded as due, at most, to the motion of  $-\text{CH}_2-\text{CH}_2-\text{CH}_2-$  parts associated with the motion of the neighbouring oxycarbonyl group, since the magnitude of the  $\gamma_d$  absorption for  $n=4$  is the largest of all the acylates examined, and it decreases continuously with increasing  $n$ . In addition to the  $\gamma_d$  process, we have to state the existence of the  $\gamma'_d$  process, instead of  $\gamma_{d'}$  in the propionate. However, the  $\gamma'_d$  process is detected only as a rise in  $\epsilon''$  with increasing frequency in the lowest temperature examined. This process may be attributed to the motion involving  $-\text{CH}_2-\text{CH}_2-$  parts in addition to the oxycarbonyl group of the propionate in a similar manner as that for the  $\gamma'_m$  process.

The authors wish to thank Mr. Y. Hirabayashi (Sanyo Wood Preserving Co., Ltd.), Dr. Y. Yoshizawa (Toshiba Corp.), and Dr. M. Fukuoka (Meidensha Electric Mfg. Co., Ltd.) for the able assistance with the experimental work. We are also grateful to the Ministry of Education, Science, and Culture, Japan for the Grant-in-Aid for Scientific Research.

### References

1. N. G. McCrum, B. E. Read, and G. Williams, *Anelastic and Dielectric Effects in Polymeric Solids*, Wiley, London, 1967.
2. J. Kolariik, *Adv. Polym. Sci.*, **46**, 119 (1982).
3. G. P. Mikhailov and T. I. Borisova, *Sov. Phys. Tech. Phys.*, **3**, 120 (1958).
4. T. Morooka, M. Norimoto, T. Yamada, and N. Shiraishi, *Wood Res.* **69**, 61 (1983).
5. T. Morooka, M. Norimoto, T. Yamada, and N. Shiraishi, *J. Appl. Polym. Sci.*, **27**, 4409 (1982).
6. C. J. Malm, J. W. Mench, D. L. Kendall, and G. D. Hiatt, *Ind. Eng. Chem.*, **43**, 684 (1951).
7. G. P. Mikhailov, A. I. Artyukov, and V. A. Shevelev, *Polym. Sci. USSR*, **11**, 628 (1969).
8. S. S. Rogers and L. Mandelkern, *J. Phys. Chem.*, **61**, 985 (1957).
9. D. J. Crofton, D. M. Moncrieff, and R. A. Pethrick, *Polymer*, **23**, 1605 (1982).
10. G. P. Mikhailov, A. I. Artyukhov, and T. I. Borisova, *Polym. Sci. USSR*, **9**, 2713 (1967).
11. H. S. Sack, T. R. Cuykendall, and T. J. Woods, *Phys. Rev.*, **94**, 1414 (1954).
12. S. Saito and T. Nakajima, *Bull. Electrotech. Lab.*, **22**, 654 (1958).
13. N. Kato, H. Saito, S. Yabumoto, and R. Fujishige, *Kobunshi-Kagaku*, **19**, 95 (1962).
14. R. W. Seymour, S. Weinhold, and K. Haynes, *J. Macromol. Sci. Phys.* **B16**(3), 337 (1979).
15. J. Russel and R. G. van Kerpel, *J. Polym. Sci.*, **25**, 77 (1957).

Received September 12, 1983

Accepted April 16, 1984